

# **<sup>18</sup>F-FESB: Automated radiosynthesis, imaging and $\beta$ -amyloid plaque studies of a novel <sup>18</sup>F-labeled PET tracer in transgenic mice with Alzheimer's Disease** Piyush Kumar<sup>1</sup>, Weizhong Zheng<sup>2</sup>, Stephen A. McQuarrie<sup>1,2\*</sup>, Jack H. Jhamandas<sup>3</sup> and Leonard I. Wiebe<sup>2</sup>

Diivision of Oncologic Imaging, Cross Cancer Institute, Edmonton, Alberta, Canada T6G 1Z2, <sup>2</sup>Faculty of Pharmacy and Pharmaceutical Sciences, Edmonton, Alberta, Canada T6G 2N8,

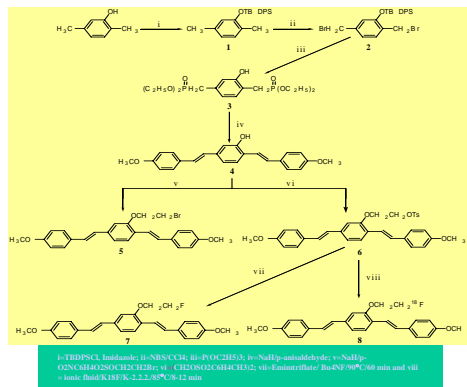
<sup>3</sup>Department of Medicine (Neurology) and Centre for Alzheimer and Neurodegenerative Research, University of Alberta, Edmonton, Alberta, Canada T6G 2S

*In spite of recent advances in new radiopharmaceuticals for the evaluation of Alzheimer's disease (AD), positron emission tomography (PET) and single photon emission tomography (SPECT) are not currently in routine use. The significant roles of amyloid cascades and neurofibrillary tangles (NFTs) in the pathogenesis of AD necessitate the development of a biomarker that facilitates early diagnosis of the disease, allows clinic-pathological correlations of amyloid deposition at an early stage and is receptor specific so that it serves as a true diagnostic tool for anti-amyloid therapies (1-3). A recent study suggests that anti-amyloid therapies, when co-investigated in combination with positron emission tomography (PET) or single photon emission computed tomography (SPECT) amyloid imaging tracers, could facilitate in vivo evaluation of the efficacy of therapy in the aging human brain. Earlier  $\beta$ -amyloid plaques related PET tracers for detecting the progression of Alzheimer's disorder include [<sup>11</sup>C]-labelled Congo Red and [<sup>99m</sup>Tc]-Chrysamine-G analogs (4) and <sup>11</sup>C-Methoxy X04 and suffer from marginal brain entry and low radiochemical yields (5-8) which consequently makes the detection of the disease difficult. <sup>11</sup>C-labeled radiopharmaceuticals also impose the risk of heavy total body radiation dose due to their short half life. Present work describes a structural modification of methoxy X04 to overcome these problems where a radioactive fluorine is incorporated nucleophilically to produce a high specific activity radiopharmaceutical. Preliminary data on ionic fluid assisted radiofluorination of <sup>18</sup>F-FESB and its PET imaging studies in transgenic Alzheimer's mouse.*

## EXPERIMENTAL

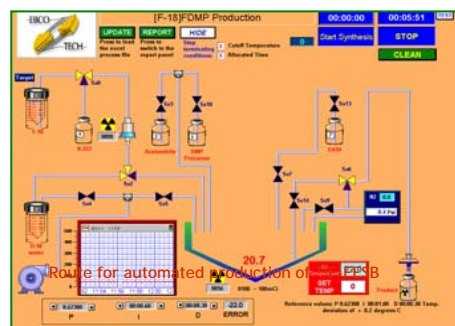
### a) Chemistry:

The synthesis of 1-(2'-fluoroethoxy)-2,5-bis(4'-methoxystyryl)benzene 7 and its tosylate precursor started with 1-O-tert-butyl(diphenylsilyl)-2,5-dimethylphenol 1 (Scheme 1). 2,5-Dimethylphenol was silylated with tert-butyl(diphenyl)silane in anhydrous pyridine since it withstands the hard acidic conditions that exist during the bromination step. Bromination of the methyl groups at C-2 and C-5, using N-bromosuccinimide, proceeded through a free radical mechanism that was assisted by benzoyl peroxide, to afford 1-((tert-butyl(diphenyl)silyloxy)-2,5-bis(bromomethyl)benzene 2 in 48% yield. Reaction of the bromomethyl product 2 at 85°C, with triethylphosphite gave 1-((tert-butyl(diphenyl)silyloxy)-2,5-bis(diethylphosphonomethyl)benzene 3 in satisfactory yield (61%). The conversion of this diethylphosphonate derivative 3 to the corresponding 2,5-bis(4-methoxystyryl)phenol, 4, progressed smoothly (74% yield). Tosylation of the free hydroxyl group using 1,2-bis(toluenesulfonyloxy)ethane in anhydrous dimethylformamide afforded 1-(2'-toluenesulfonyloxy)-2,5-bis(4'-methoxystyryl)benzene 6 as a yellow solid in 48% yield. The tosylate 6, on reaction with tetrabutyl ammonium fluoride at 100°C, gave 1-(2'-fluoroethoxy)-2,5-bis(4'-methoxystyryl)benzene, 7, in 9% yield.



### b) Radiofluorination:

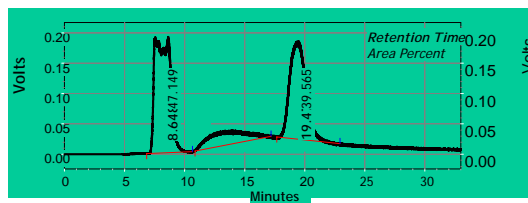
- The synthesis of <sup>18</sup>F labeled 8 was performed in an automated synthesis unit (ASU), initially using the conventional method of Kryptofix 2.2.2/K<sup>18</sup>F complex assisted radiofluorination at elevated temperatures, but this provided low radiochemical yields (3-5%).
- Use of an appropriate ionic fluid in our radiofluorination reactions led to significant improvement in the labeling efficiency of <sup>18</sup>F-FESB (table 1).
- A typical radiofluorination reaction involved reaction of tosylate precursor (4-6 mg) with K-2.2.2/radiofluoride complex (20 mg/60-70 GBq) in anhydrous acetonitrile (2 mL) and dimethylformamide (50  $\mu$ L) at 110°C for 8-12 min in the presence of desired 'ionic fluid' (50  $\mu$ L). The labeled product, after removal of the solvents was pushed out of the ASU with 1.5 mL of clinical grade ethanol and purified on a reversed phase HPLC to obtain pure <sup>18</sup>F-FESB.



### c) HPLC Purification:

HPLC chromatography was performed to purify <sup>18</sup>F-FESB and determine its specific activity. It involved the use of a Whatman reverse phase C-18 column (30 x 0.9 cm) as a stationary phase and EtOH:H<sub>2</sub>O (75:25; v/v) as mobile phase. The elution was done at a flow rate of 1.5 mL/min. Auto-Scaled UV and radio chromatograms of <sup>18</sup>F-FESB were archived. A typical HPLC analysis of <sup>18</sup>F-FESB labeled mixture is shown in the chromatogram below.

- <sup>18</sup>F-FESB appears at 19.4 min (radio-chromatogram) (it lags by ~0.4 min since the radio detector is attached after the UV detector).
- The retention times for emimtriflate and bmmetrafluoroborate are 7.3 and 6.9 min respectively, therefore, the radioactive peaks appearing between 7-10 min in the radiochromatogram of the labeled <sup>18</sup>F-FESB mixture correspond to unreacted fluoride, radiofluorinated emimtriflate and bmmetrafluoroborate (depending on the ionic solvent used in radiofluorination) salts formed due to the exchange of radioactive fluorine and unreacted ionic fluid.
- An uncharacterized radioactive hump appearing between 11-18 min is visible in the chromatogram (Fig. 1) but the purity of <sup>18</sup>F-FESB is not compromised during HPLC purification of the reaction mixture by collecting <sup>18</sup>F-FESB after 30 sec of the peak start.



HPLC Chromatogram of <sup>18</sup>F-FESB Reaction Mixture

## RESULTS

### Radiofluorination reaction parameters for <sup>18</sup>F-FESB

Reaction #	Ionic Fluid*	Amount	Reaction Time	Purified RCY ( $\mu$ L)	Specific Activity (min)	(%)	(Ci/ $\mu$ M)
1	BmimBF4	20	12	16.9			
2	BmimBF4	20	8	43.2			
3	BmimBF4	50	9	76.9			
4	Emimtriflate	50	8	39.6			>40
5	Emimtriflate	50	8	25.5			
6	Emimtriflate	50	8	42.5			
7	None	N/A	4	3.0			
8	None	N/A	8	7.0			

\*Acetonitrile (2 mL) and anhydrous DMF (50  $\mu$ L) were used as reaction solvent during the radiolabeling.

### Digital Phosphor-imaging Studies:

*In vitro* binding of <sup>18</sup>FESB to mouse AD plaques (phosphor imaging): 15 min (right in each image) & 30 min (left in each image) post-incubation with 0.2 MBq (left) and 0.6 MBq (right) of <sup>18</sup>FESB.



### PET Imaging:



Figure a PET scan of a transgenic AD mouse using a) <sup>18</sup>F-FESB and b) <sup>18</sup>F-FDG

### CONCLUSION

The synthesis of <sup>18</sup>F-FESB, a fluorinated Congo red derivative was developed using an ASU. Use of 'ionic fluids' in the radiochemical synthesis significantly enhanced the labeling efficiency of the product. An attempt to correlate radiochemical yield of 8 to varying amounts of the ionic fluids bmmimBF4 or emimtriflate were inconclusive since correlations between these two parameters were not evident. <sup>18</sup>F-FESB, being a fluorinated analog, has much longer half life than other <sup>11</sup>C-labeled members of this class and, therefore, will have a direct impact on the patients radiation doses and delineation of  $\beta$ -amyloid plaques from other regions in the brain. In vitro studies of mouse AD brain with <sup>18</sup>F-FESB using digital phosphorimaging shows accumulation of radioactivity in the inner brain area indicating its uptake by  $\beta$ -amyloid plaques. Congo Red staining of human AD brain tissues incubated with <sup>18</sup>F-FESB shows its specific binding to  $\beta$  plaques. Initial PET imaging studies in AD mice with <sup>18</sup>F-FESB show faint but specific uptake in the brain region.

**ACKNOWLEDGEMENTS** The authors gratefully acknowledge the Alberta Cancer Board and the University of Alberta Hospital Foundation for their financial support.